Institute of
Applied Mechanics
Institut für Baumechanik

TU Graz
Graz University of Technology

Preprint Series

Institute of Applied Mechanics

Graz University of Technology

Preprint No 4/2010

Wave Propagation in a One Dimensional Partially Saturated Poroelastic Column

Peng Li, Martin Schanz
Institute of Applied Mechanics, Graz University of Technology

Accepted for publication in: *Geophysical Journal International*
The definitive version is available at www.blackwell-synergy.com
Latest revision: December 1, 2010

Abstract

Based on the theory of mixtures, a dynamic three phase model for partially saturated poroelasticity is established. This model is applied to a one dimensional column and an analytical solution in the Laplace domain is deduced. By using the convolution quadrature method the solution in the time domain is obtained. Using the material data of Massillon sandstone the three different compressional waves, the fast wave, the second slow wave, and the third slow wave, are calculated and validated with the Biot-Gassmann prediction. The wave propagation behavior in terms of displacement and pore pressure is also examined with the analytical solution. By neglecting the viscous behavior of the interaction between the fluids and the solid the second and the third slow compressional waves are identified.

1 Introduction

Wave propagation in porous media is important, e.g. in natural formations as soft rock, soil, and tissue, or artificial materials as cement. For saturated porous media there are in principle three similar theories available – that of Biot [5, 6], the Theory of Porous Media (e.g. [8]), and the simple mixture theory [29]. The latter ones are based on the principles of continuum mechanics and the mixture theory. Their extension to the partially saturated case may be found in [13]. Another approach for porous media like rocks is the double porosity model based on Biot's theory [30].

For partially saturated porous media, Philippacopoulos [17] studied a "partially" saturated poroelastic half-space problem, where exact analytical expressions have been obtained for the propagation due to a point load acting vertically at the surface of a medium that consists of a dry-type layer overlying a fluid-saturated porous substratum. Zienkiewicz et al. [31] extended the formulation of static and dynamic saturated soils to problems of semi-saturated behaviour with the assumption of free air ingress. Berryman [4] derived the equations of poroelasticity for partially saturated materials by using the physically reasonable assumption of negligible capillary pressure change during passage of an acoustic signal through the media. Smeulders et al. [24] studied the propagation of the compressional waves in a porous medium for a pore liquid containing a small volume fraction of gas. Further, the effect of oscillating gas bubbles was taken into account by introducing a frequency-dependent fluid bulk modulus, which was incorporated in Biot's theory. A poroelastic model using the theory of mixture with interfaces, which can be used to analyze the propagation conditions and characteristics of acoustical waves in unsaturated porous media has been published by Muraleetharan and Wei [14] (see also [27, 28]). Schrefler and Scotta [23] presented a fully coupled dynamic model for the analysis of water and air flow in deforming porous media under fully or partially saturated conditions. They discussed the drainage problem of a soil column, the air storage problem in an aquifer, and the dynamic analysis of a sand column subjected to a step load. Gatmiri and Jabbari [11, 12] published the closed form two and three dimensional Green's functions of the governing differential equations for an unsaturated deformable porous medium. Albers [1, 2] investigated the propagation of sound waves in partially saturated soils with a macroscopic linear model, which was based on the two component model of Biot and on the Simple Mixture Model by Wilmanski [29]. In these works, a porous medium consisting of a deformable skeleton and two compressible, chemically non-reacting, pore fluids (liquid and gas) has been modelled, and a spectral analysis of wave propagation in partially saturated porous media is performed for more than twenty sorts of soils. Ravichandran and Muraleetharan [19] compared the complete and reduced Finite Element formulations for an unsaturated soil. The permanent deformations were predicted taking elastoplastic effects into account.

The analytical solution of wave propagation in saturated porous media has been deduced by Garg et al. [9]. There are also other 1-d solutions available which can be found in the review article [21]. However, for other than saturated models there are not too many 1-d solutions available. It may only be mentioned the solution by Vgenopoulou and Beskos [26] based on the double porosity model.

In the present work, the solution of a finite one dimensional column with Neumann and Dirichlet boundary conditions are deduced based on the theory of mixtures. The solution is obtained in the Laplace domain and the convolution quadrature method is chosen to obtain the time domain solution. The material data of Massillion sandstone are used in the example. The column response to the dynamic loading is examined in terms of phase velocities, displacement, pore water pressure, and pore air pressure. One of the significant findings of BiotâĂŹs theory of poroelasticity is the identification of three waves for a three dimensional continuum, two compressional waves and one shear wave. The first compressional wave is very similar to the compressional wave in an elastic medium, while the second wave, also named BiotâĂŹs second slow wave, has a strongly dispersive character and has been experimentally confirmed by [18]. Due to the existence of the second pore fluid in the partially saturated case, an additional third compressional wave emerges. In this paper, under special conditions, the creation and propagation of the second and third slow compressional waves can be clearly observed. With the present solution, it is possible to simulate a column response under a wide range of transient loading conditions, and the solution can be used to validate numerical simulation results.

Throughout this work, the indical notation is used. The summation convention is applied over repeated indices and Latin indices receive the values 1, 2, 3 in three dimensions and 1, 2 in two dimensions. Commas $()_{,i}$ denote spatial derivatives and ∂_t the time derivative. δ_{ij} denotes the Kronecker delta, i.e. $\delta_{ij} = 1$ for $i = j$ else $\delta_{ij} = 0$ holds. The Laplace transform of a function $f(t)$ is denoted by $\hat{f}(s)$ with the complex Laplace parameter $s \in \mathbb{H}$ and $\mathbb{H} = \{s \in \mathbb{C} | \Re(s) > 0\}$.

2 Governing equations

For dynamic partially saturated poroelasticity the governing equations are stated following the work of Lewis and Schrefler [13]. To obtain a representation with as few as possible unknowns, i.e. the solid displacements u_i, the pore wetting fluid pressure p^w, and the pore non-wetting fluid pressure p^a, the governing equations are transformed to Laplace domain to eliminate the relative fluid to solid displacements.

2.1 Constitutive assumptions

For a partially saturated porous medium, the porosity n measures the void spaces, which is the ratio of the volume of voids V_{void} over the total volume V_{total}

$$n = \frac{V_{void}}{V_{total}} . \tag{1}$$

The voids are filled with a mixture of fluids, for instance, a mixture of water and air in soil mechanics, or a mixture of oil and water in petroleum engineering. The saturation degrees are defined as the ratios of the volume occupied by the fluid V_w or V_a to the void volume, i.e. it holds

$$S_w = \frac{V_w}{V_{void}} \quad S_a = \frac{V_a}{V_{void}} \qquad S_w + S_a = 1 . \tag{2}$$

The capillary pressure p^c in a partially saturated media is given following Brooks and Corey [7]

$$p^c = p^a - p^w = p^d S_e^{-1/\vartheta} , \tag{3}$$

where p^d is the non-wetting fluid entry pressure and ϑ is the pore size distribution index. S_e denotes the effective wetting fluid saturation degree given by

$$S_e = \begin{cases} 0 & S_w \leq S_{rw} \\ \dfrac{S_w - S_{rw}}{S_{ra} - S_{rw}} & S_{rw} < S_w < S_{ra} \\ 1 & S_w \geq S_{ra} \end{cases} , \tag{4}$$

where S_{rw} is the residual wetting fluid saturation and S_{ra} is the non-wetting fluid entry saturation.

The total stress σ is expressed by

$$\sigma_{ij} = \sigma'_{ij} - \delta_{ij}\alpha(S_w p^w + S_a p^a) , \tag{5}$$

where σ' denotes the effective stress, $\alpha = 1 - K/K_s$ describes the compressibility of the solid skeleton with the drained bulk modulus of the mixture K and K_s is the bulk modulus of the solid skeleton. Assuming an elastic isotropic material for the skeleton, the constitutive model is

$$\sigma'_{ij} = (K - \frac{2}{3}G)\delta_{ij}u_{k,k} + G(u_{i,j} + u_{j,i}) , \tag{6}$$

with G denoting the shear modulus. Further, in (6) a linear stress-strain relation is assumed.

2.2 Balance equations

The balances of mass for the solid and both fluids are

$$\partial_t[(1-n)\rho_s] + (1-n)\rho_s\partial_t u_{i,i} = 0 \tag{7a}$$

$$\partial_t(nS_f\rho_f) + nS_f\rho_f\partial_t(u_{i,i} + u^f_{i,i}) = 0 \tag{7b}$$

where ρ_s and $\rho_f (f = w, a)$ denote the density of the solid and the fluids, respectively. Note that in (7b), and also in the following, with the index f the equations of both fluids are summarised. The displacements $u^f (f = w, a)$ are the relative displacement of the fluids according to the solid. The equations (7) are formulated under the assumptions that the dissolved non-wetting fluid into the wetting fluid can be neglected. Further, due to the linearization the gradients of the porosity, the densities, and the saturation degrees vanish.

Assuming a compressible solid phase and that the first stress invariant is proportional to the volumetric strain an equation for the time derivative of the porosity can be formulated (see Lewis and Schrefler [13])

$$\partial_t n - \zeta(S_{ww}\partial_t p^w + S_{aa}\partial_t p^a) + \zeta K_s\partial_t u_{i,i} = 0 , \tag{8}$$

with the abbreviations $\zeta = (\alpha - n)/K_s$, $S_{ww} = S_w + p^c\dfrac{\partial S_w}{\partial p^c}$, and $S_{aa} = S_a - p^c\dfrac{\partial S_w}{\partial p^c}$. Inserting S_e of (4) in (3) the derivative of the fluid saturation with respect to the capillary pressure can be calculated. Combining this with the capillary pressure of (3) yields

$$p^c\frac{\partial S_w}{\partial p^c} = -\vartheta(S_w - S_{rw}) . \tag{9}$$

Inserting the equations (8) and (9) in the mass balance of both fluid parts (7b) results in the two continuity equations

$$\alpha S_w \partial_t u_{i,i} + (\zeta S_{ww} S_w + \frac{n}{K_w} S_w - S_u)\partial_t p^w + (\zeta S_{aa} S_w + S_u)\partial_t p^a + nS_w \partial_t u^w_{i,i} = 0 \tag{10a}$$

$$\alpha S_a \partial_t u_{i,i} + (\zeta S_{ww} S_a + S_u)\partial_t p^w + (\zeta S_{aa} S_a + \frac{n}{K_a} S_a - S_u)\partial_t p^a + nS_a \partial_t u^a_{i,i} = 0 \ , \tag{10b}$$

with $S_u = -\frac{\vartheta(S_{ra} - S_{rw})}{p^d} \left(\frac{S_w - S_{rw}}{S_{ra} - S_{rw}}\right)^{\frac{\vartheta+1}{\vartheta}}$.

Next, the balances of momentum have to be formulated. Instead of the balance for the solid that of the mixture is used. Beside this, the two fluid balances are used. Taking into account the constitutive assumption for the total stress (5) this gives

$$Gu_{i,jj} + (K + \frac{1}{3}G)u_{j,ij} - \alpha(S_w p^w_{,i} + S_a p^a_{,i}) + F_i = \rho \partial_t^2 u_i + nS_w \rho_w \partial_t^2 u^w_i + nS_a \rho_a \partial_t^2 u^a_i \tag{11a}$$

$$nS_f \partial_t u^f_i = -\kappa_f \left(p^f_{,i} + \rho_f \partial_t^2 u_i + \rho_f \partial_t^2 u^f_i\right) \tag{11b}$$

with the bulk body force F_i. The bulk density denoted by $\rho = (1-n)\rho_s + nS_w\rho_w + nS_a\rho_a$ is the averaged density of the mixture. The phase permeabilities of the wetting fluid ($f = w$) and the non-wetting fluid ($f = a$) is $\kappa_f = \frac{K_{rf} k}{\eta_f}$ ($f = w,a$). Beside the relative fluid phase permeability K_{rf}, k is the intrinsic fluid permeability, and η_f is the viscosity of the fluid. The relative phase permeability K_{rf} can be evaluated either following Brooks and Corey [7] or van Genuchten [25]. In the following, Brooks' equations are used

$$K_{rw} = S_e^{(2+3\vartheta)/\vartheta} \qquad K_{ra} = (1-S_e)^2[1 - S_e^{(2+\vartheta)/\vartheta}] \ . \tag{12}$$

2.3 Governing equations in the Laplace domain

The equations (10) and (11) are sufficient to solve the problem of unsaturated poroelasticity. Counting the unknown field variables shows that there is another choice which uses less variables. It would be natural to describe the solid by the displacements and the fluids by the pressures. However, the elimination of the relative displacements is not possible in time domain because it appears above in different orders of time derivatives. Hence, these equations are transformed to Laplace domain to extract the relative displacements.

With the definition of the Laplace transformation

$$\hat{f}(s) = \mathcal{L}\{f(t)\} = \int_0^\infty e^{-st} f(t) dt \tag{13}$$

the momentum balances of the fluids are

$$nS_f \hat{u}^f_i s = -\kappa_f \left(\hat{p}^f_{,i} + \rho_f \hat{u}_i s^2 + \rho_f \hat{u}^f_i s^2\right) \ . \tag{14}$$

Reorganizing both equations in (14) with respect to the respective relative displacement gives the fluxes

$$q_i^w = s\hat{u}_i^w = -\beta \frac{1}{n\rho_w s}\left(\hat{p}^w_{,i} + \rho_w s^2 \hat{u}_i\right) \qquad \text{with} \quad \beta = \frac{\kappa_w n \rho_w s}{nS_w + \kappa_w \rho_w s} \tag{15a}$$

$$q_i^a = s\hat{u}_i^a = -\gamma \frac{1}{n\rho_a s}\left(\hat{p}^a_{,i} + \rho_a s^2 \hat{u}_i\right) \qquad \text{with} \quad \gamma = \frac{\kappa_a n \rho_a s}{nS_a + \kappa_a \rho_a s}\ . \tag{15b}$$

Substituting the relative displacements (15) in the transformed balance of momentum of the mixture (11a) and both continuity equations (10) results in the governing equations in the Laplace domain

$$G\hat{u}_{i,jj} + (K + \frac{G}{3})\hat{u}_{j,ij} - (\rho - \beta S_w \rho_w - \gamma S_a \rho_a)s^2 \hat{u}_i - (\alpha - \beta) S_w \hat{p}^w_{,i} - (\alpha - \gamma) S_a \hat{p}^a_{,i} = -\hat{F}_i \tag{16a}$$

$$(\alpha - \beta) S_w s \hat{u}_{i,i} + (\zeta S_{ww} S_w + \frac{n}{K_w} S_w - S_u) s\hat{p}^w - \frac{\beta S_w}{\rho_w s}\hat{p}^w_{,ii} + (\zeta S_{aa} S_w + S_u) s\hat{p}^a = 0 \tag{16b}$$

$$(\alpha - \gamma) S_a s \hat{u}_{i,i} + (\zeta S_{ww} S_a + S_u) s\hat{p}^w + (\zeta S_{aa} S_a + \frac{n}{K_a} S_a - S_u) s\hat{p}^a - \frac{\gamma S_a}{\rho_a s}\hat{p}^a_{,ii} = 0 \tag{16c}$$

with the unknowns solid displacement $\hat{u}_i$, pore fluid pressure $\hat{p}^w$ and $\hat{p}^a$.

3 Analytical solution

To study the influence of partially saturated poroelastic parameters on wave propagation, a one dimensional column of length ℓ is considered. It is assumed that the side walls of the column are rigid, frictionless, and impermeable. Due to these restrictions only the vertical displacement u, the pore pressures p^w and p^a remain as the degrees of freedom. At the top of the column, a stress $\sigma = -S_0 H(t)$, a pressure $p^w = P^w H(t)$, and a pressure $p^a = P^a H(t)$ are prescribed (see Figure 1). Therein, $H(t)$ denotes the unit step function in time, i.e. the load is applied at $t > 0$. The bottom is modelled impermeable and it might move with a constant displacement $u = U_0 H(t)$. This one dimensional example can also be seen as an approximation of a partially saturated poroelastic half space with an infinite layer width.

For the above assumption, and with a vanishing body force term, the governing equations are reduced to three scalar coupled ordinary differential equations

$$(K + \frac{4}{3}G)\hat{u}_{,yy} - s^2(\rho - \beta S_w \rho_w - \gamma S_a \rho_a)\hat{u} - (\alpha - \beta) S_w \hat{p}^w_{,y} - (\alpha - \gamma) S_a \hat{p}^a_{,y} = 0 \tag{17a}$$

$$(\alpha - \beta) S_w s \hat{u}_{,y} + (\zeta S_{ww} S_w + \frac{n}{K_w} S_w - Su) s\hat{p}^w - \frac{\beta S_w}{\rho_w s}\hat{p}^w_{,yy} + (\zeta S_{aa} S_w + S_u) s\hat{p}^a = 0 \tag{17b}$$

$$(\alpha - \gamma) S_a s \hat{u}_{,y} + (\zeta S_{ww} S_a + S_u) s\hat{p}^w + (\zeta S_{aa} S_a + \frac{n}{K_a} S_a - S_u) s\hat{p}^a - \frac{\gamma S_a}{\rho_a s}\hat{p}^a_{,yy} = 0\ , \tag{17c}$$

with the boundary conditions in the Laplace domain

$$\begin{array}{lll} \hat{u}(y=0) = U_0 & \hat{q}^w(y=0) = 0 & \hat{q}^a(y=0) = 0 \\ \hat{\sigma}(y=\ell) = -S_0 & \hat{p}^w(y=\ell) = P^w & \hat{p}^a(y=\ell) = P^a\ . \end{array}$$

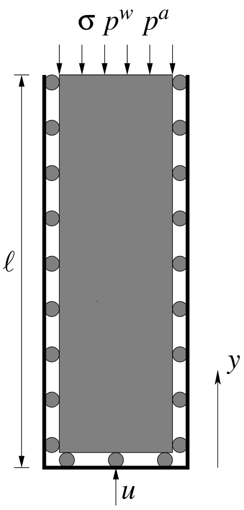

Figure 1: A one dimensional column under dynamic loads

This turns out to be a system of homogeneous ordinary differential equations with inhomogeneous boundary conditions. Such a system can be solved by using the exponential ansatz

$$\hat{u}(y) = Ue^{\lambda sy} \quad \hat{p}^w(y) = U^w e^{\lambda sy} \quad \hat{p}^a(y) = U^a e^{\lambda sy} \,. \tag{18}$$

Inserting the ansatz into equations (17) results in an eigenvalue problem for λ

$$\begin{bmatrix} (B_1\lambda^2 - B_2)s & -B_3\lambda & -B_4\lambda \\ B_3\lambda s & (B_5 - B_6\lambda^2) & B_7 \\ B_4\lambda s & B_8 & (B_9 - B_{10}\lambda^2) \end{bmatrix} \begin{bmatrix} U \\ U^w \\ U^a \end{bmatrix} = 0 \quad , \tag{19}$$

with the characteristic equation

$$C_1\lambda^6 + C_2\lambda^4 + C_3\lambda^2 + C_4 = 0 \,. \tag{20}$$

The six complex roots of equation (20) corresponds to the three compressional waves in the 1-d unsaturated poroelastic medium and are given by

$$\lambda_1 = -\lambda_4 = \sqrt{N_1 + \frac{N_2C_2^2}{3C_1} - N_2C_3 + \frac{1}{3N_2C_1}} \tag{21a}$$

$$\lambda_2 = -\lambda_5 = \sqrt{N_1 + \frac{3C_1C_3 - C_2^2}{6C_1}N_2(1 - i\sqrt{3}) - \frac{1}{6N_2C_1}(1 + i\sqrt{3})} \tag{21b}$$

$$\lambda_3 = -\lambda_6 = \sqrt{N_1 + \frac{3C_1C_3 - C_2^2}{6C_1}N_2(1 + i\sqrt{3}) - \frac{1}{6N_2C_1}(1 - i\sqrt{3})} \,. \tag{21c}$$

The abbreviations B_i, C_i, and N_i can be found in the appendix A.

Corresponding to the six roots the six solutions for the ansatz in (18) can be super-imposed. This leads to the complete solution of the homogeneous problem

$$\hat{u}(y) = \sum_{i=1}^{6} U_i e^{\lambda_i s y} \qquad \hat{p}^w(y) = \sum_{i=1}^{6} U_i^w e^{\lambda_i s y} \qquad \hat{p}^a(y) = \sum_{i=1}^{6} U_i^a e^{\lambda_i s y} \; . \tag{22}$$

According to (19), the relationships between U_i and U_i^w, and U_i and U_i^a are

$$U_i^w = \frac{(B_1 B_7 + B_3 B_4 S_a)\lambda_i^2 - B_2 B_7}{(B_4 B_6 S_a \lambda_i^2 + B_3 B_7 S_w - B_4 B_5 S_a)\lambda_i} s U_i = a_i s U_i \tag{23a}$$

$$U_i^a = \frac{(B_1 B_8 + B_3 B_4 S_w)\lambda_i^2 - B_2 B_8}{(B_3 B_{10} S_w \lambda_i^2 + B_4 B_8 S_a - B_3 B_9 S_w)\lambda_i} s U_i = b_i s U_i \; . \tag{23b}$$

By substituting U_i^w and U_i^a with U_i in equation (22) the solutions are

$$\hat{u}(y) = \sum_{i=1}^{6} U_i e^{\lambda_i s y} \qquad \hat{p}^w(y) = \sum_{i=1}^{6} a_i s U_i e^{\lambda_i s y} \qquad \hat{p}^a(y) = \sum_{i=1}^{6} b_i s U_i e^{\lambda_i s y} \; . \tag{24}$$

Rewriting the boundary conditions with the ansatz functions (18) and the relations (23) six conditions for the six unknown values U_i are available. Following the definition of the total stress tensor (5), the stress boundary condition at the top of the column $(y = \ell)$ is

$$(K + \frac{4}{3}G) s \sum_{i=1}^{6} (\lambda_i e^{\lambda_i s \ell} U_i) = [\alpha(S_w P^w + S_a P^a) - S_0] \tag{25}$$

and at the same location the pressure boundary conditions are

$$s \sum_{i=1}^{6} (a_i e^{\lambda_i s \ell} U_i) = P^w \qquad s \sum_{i=1}^{6} (b_i e^{\lambda_i s \ell} U_i) = P^a \; . \tag{26}$$

On the bottom of the column $(y = 0)$ the fluxes and the displacement are prescribed, which yields

$$\sum_{i=1}^{6} (a_i \lambda_i U_i) = -\rho_w U_0 \qquad \sum_{i=1}^{6} (b_i \lambda_i U_i) = -\rho_a U_0 \tag{27}$$

and

$$\sum_{i=0}^{6} U_i = U_0 \; . \tag{28}$$

After determining the six constants U_i with the above six conditions the solutions in Laplace domain are known.

The solutions can be divided into four different load cases based on the superposition principle. The solution for the stress boundary condition ($\hat{u}|_{y=0} = 0$, $\hat{\sigma}|_{y=\ell} = -S_0$, $\hat{p}^w|_{y=\ell} = 0$,

$\hat{p}^a|_{y=\ell} = 0$) is

$$\hat{u} = \frac{S_0 s^{-1}}{M(K+\frac{4}{3}G)} \sum_{i=1}^{3} \left[\frac{e^{-\lambda_i s(y+\ell)} - e^{\lambda_i s(y-\ell)}}{1+e^{-2\lambda_i s\ell}} t_i \right] \tag{29a}$$

$$\hat{p}^w = \frac{S_0}{M(K+\frac{4}{3}G)} \sum_{i=1}^{3} \left[\frac{e^{-\lambda_i s(y+\ell)} + e^{\lambda_i s(y-\ell)}}{1+e^{-2\lambda_i s\ell}} t_i a_i \right] \tag{29b}$$

$$\hat{p}^a = \frac{S_0}{M(K+\frac{4}{3}G)} \sum_{i=1}^{3} \left[\frac{e^{-\lambda_i s(y+\ell)} + e^{\lambda_i s(y-\ell)}}{1+e^{-2\lambda_i s\ell}} t_i b_i \right] , \tag{29c}$$

with $t_1 = a_2b_3 - a_3b_2$, $t_2 = a_3b_1 - a_1b_3$, $t_3 = a_1b_2 - a_2b_1$, and $M = t_1\lambda_1 + t_2\lambda_2 + t_3\lambda_3$. The corresponding stress and fluxes can be calculated following the definitions in (5) and (15). The solutions for the other three load cases can be found in appendix B.

As β and γ are dependent of the Laplace parameter s, the roots λ_i and consequently a_i and b_i are also dependent on s. Therefore, an analytical inverse Laplace transform of the solutions above is generally not possible. However, if the viscosity of the fluids is neglected, i.e. the permeability tends to infinity, an analytical inverse Laplace transform can be found following the lines in [22]. However, for arbitrary values of the permeability, a numerical inverse Laplace transform is needed. A number of methods to determine the inverse Laplace transform are available in the literature. Here, the convolution quadrature method (CQM) is employed

$$u(n\Delta t) = \sum_{k=0}^{n} \omega_{n-k}(\Delta t) g(k\Delta t), n = 0, 1, ..., N , \tag{30}$$

with the weights function $\omega_{n-k}(\Delta t)$ determined by

$$\omega_{n-k}(\Delta t) = \frac{\mathscr{R}e^{-(n-k)}}{L} \sum_{\ell=0}^{L-1} \hat{u}\left(\frac{\gamma(\mathscr{R}e^{i\ell\frac{2\pi}{L}})}{\Delta t} \right) e^{-i(n-k)\ell\frac{2\pi}{L}} . \tag{31}$$

For details on the application of the CQM see [20]. In the following calculations, a BDF2 as underlying multistep method $\gamma(z)$ and $\mathscr{R}^N = 10^{-5}$ is used.

4 One dimensional wave propagation

Wave propagation in an one dimensional partially saturated poroelastic column is studied in the following using the developed analytical solution. To be confident of the solution, validations of the phase velocities with experiments [15, 16] and the displacement and the pore pressure solutions with analytical solutions of special cases [10, 22] are performed. The material data of Massilon sandstone measured by Murphy [16] are used in the calculations. Hence, the fluids are water and air. These data are given in Table 1. The pore size distribution index ϑ is set to 1.5, the residual water saturation S_{rw} is set to 0, and the air entry saturation S_{ra} is set to 1. The two latter values are somehow arbitrary but enables to evaluate the solutions also in this extreme cases. This is done only for comparison reasons.

Table 1: Parameters of Massilon sandstone

Parameter type	Symbol	Value	Unit
Porosity	n	0.23	-
Density of the solid skeleton	ρ_s	2650	kg/m^3
Density of the water	ρ_w	997	kg/m^3
Density of the air	ρ_a	1.10	kg/m^3
Drained bulk modulus of the mixture	K	1.02×10^9	N/m^2
Shear modulus of the mixture	G	1.44×10^9	N/m^2
Bulk modulus of the solid skeleton	K_s	3.5×10^{10}	N/m^2
Bulk modulus of the water	K_w	2.25×10^9	N/m^2
Bulk modulus of the air	K_a	1.10×10^5	N/m^2
Intrinsic permeability	k	2.5×10^{-12}	m^2
Viscosity of the water	η_w	1.0×10^{-3}	Ns/m^2
Viscosity of the air	η_a	1.8×10^{-5}	Ns/m^2

First, the wave velocities are controlled. In the model, there are three compressional waves – the fast wave p_1, the second slow wave p_2, and the third slow wave p_3. The shear wave is also included in section 2 but not in the 1-d model. The wave speeds and the attenuations are calculated from the complex roots λ_i of equation (20). Taking the Laplace parameter $s = i\omega$, i.e., the real part is set to zero, the real part of λ_i represents the phase velocities v_p and the attenuation a_p is (see [1])

$$v_{pi} = \frac{1}{\Re(\lambda_i)} \qquad a_{pi} = \omega\Im(\lambda_i)\ . \tag{32}$$

These velocities and attenuations are plotted versus the saturation degree in Figure 2 for different frequencies ω. The fast compression wave speed v_{p1} is compared to Gassmann's equations

$$K^* = K + \frac{\alpha^2}{\frac{\alpha-n}{K_s} + n(\frac{S_w}{K_w} + \frac{S_a}{K_a})} \qquad v_p^G = \sqrt{\frac{K^* + \frac{4}{3}G}{\rho}}\ , \tag{33}$$

where K^* is the effective bulk modulus of the undrained fluid mixture of a saturated porous medium. Murphy [16] tested the Massillon sandstone and verified Gassmann's prediction. Hence, the dots in Figure 2a are also verified by experiment. The known effect that the fast wave velocity v_{p1} decreases with increasing the water saturation is visible, as well as the drastic increase for the nearly saturated case. This result matches Gassmann's predictions. According to them, with increasing the water saturation the averaged mixture density ρ increases and this slows down v_p. The effective bulk modulus K^* also increases and this speeds up v_p. However, for the air phase, since K_a is very small compared to K_w, K^* will not change too much until S_w increases to some value, i.e., $S_w = 0.999$, when K^* increases rapidly. In other words, for large values of saturation, generally, the fast wave velocity will increase rapidly corresponding to the increase of saturation, which can be concluded from equation (33). Besides, the fast wave is almost frequency independent. Only when the water saturation is very close to 1 there exist tiny differences of the wave velocity for different frequencies.

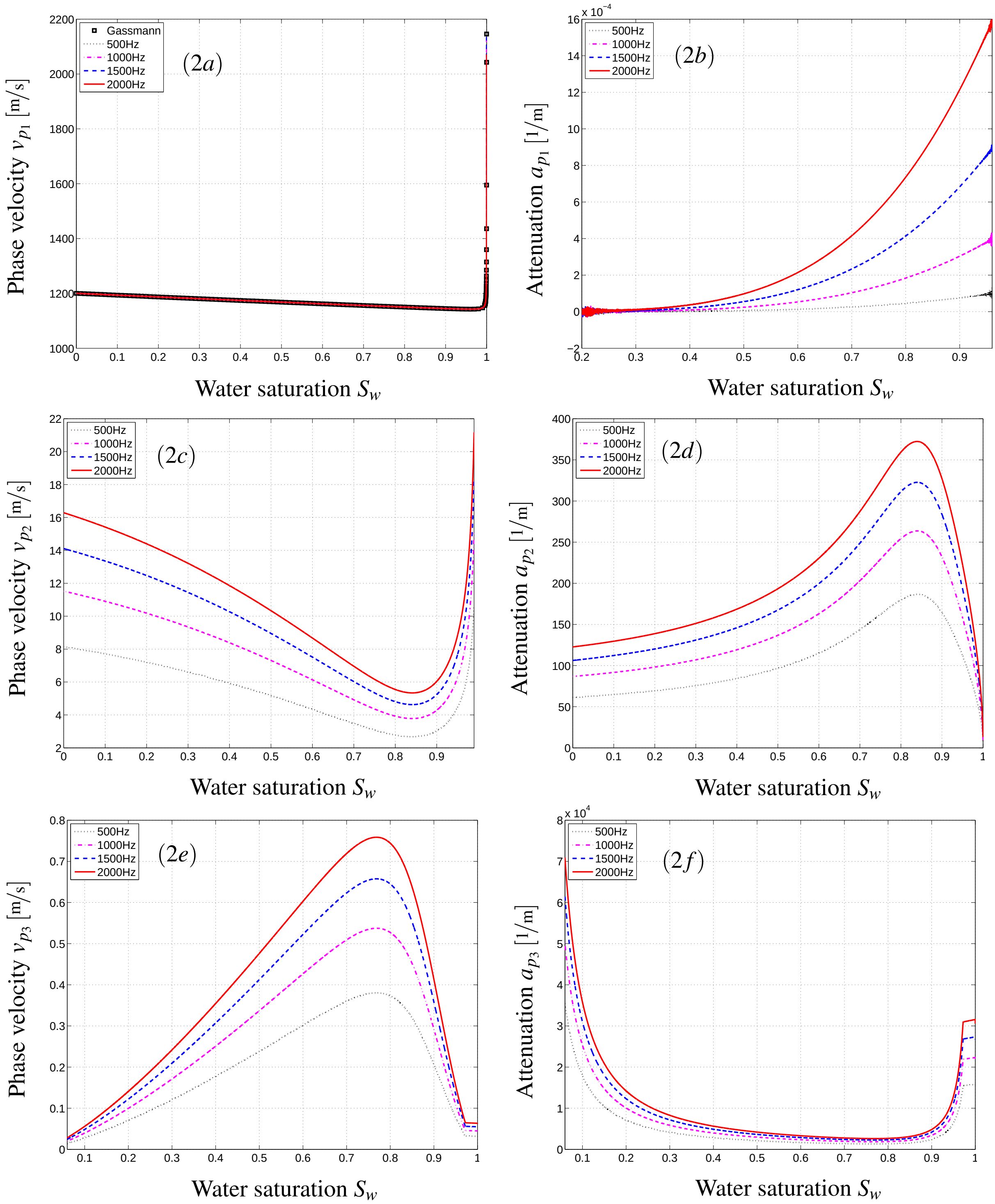

Figure 2: The fast, the second slow, and the third slow compressional wave velocities and attenuations versus water saturation

The second and the third slow waves are much slower compared to the fast wave. The second slow wave velocity v_{p_2} decreases with increasing the saturation degree to the value 0.85, then it increases very fast. The third slow wave velocity v_{p_3} increases with increasing the saturation degree to the value 0.75, then it decreases very fast. Both slow waves are frequency dependent and the wave velocities increase with increasing the frequency. This fits to the results of Albers [1] and can be understood if the different states of the fluids combinations are considered. Bao et al. [3] summarized the different features for the four air phase patterns:

1. Wholly continuous stage ($S_w < 0.55$), where the moisture only exists in the smaller voids and the water is not necessarily interconnected, the air phase is continuous in the soil mass and connected to the atmosphere.

2. Partially continuous stage ($0.55 \leq S_w \leq 0.85$), where the moisture will gradually occupy all the smaller pore passageways, the air phase is accumulating in the larger voids and it is still connected to the atmosphere.

3. Internally continuous stage ($0.85 \leq S_w \leq 0.90$), where the water will begin to occupy the larger pore passageways and seal off the boundary voids of the soil mass, the air phase is not connected to the atmosphere, but inside the soil mass it remains to be connected.

4. Completely sealed stage ($S_w > 0.90$), where the water with occluded air bubbles occupy all the pore passageways, the air phase will appear only in the form of occluded air bubbles suspended in and moving with the water.

Based on these considerations it is clear why there is a turning point for both phase velocities.

The attenuation of the fast wave is extremely small and may be neglected. This is the reason that the fast wave is always easy to detect. On the other hand, the attenuation of the two slow waves is very large, especially for the third slow wave, the value can be as high as $7 \times 10^4\,{}^1\!/\mathrm{m}$. The two slow waves are highly damped caused by the viscous interaction of the fluids with the solid and the suction effect. The attenuation of all the three waves is frequency dependent and the attenuation becomes higher with increasing the frequency.

After controlling the wave behavior and with this in principle the model, next, the displacement and the pore pressure are studied. The time domain results are calculated by using the convolution quadrature method as mentioned before by choosing the time step size to $\Delta t = 1 \times 10^{-5}\,\mathrm{s}$. Assuming the values $S_0 = 1\,\mathrm{N/m^2}$ and $\ell = 10\,\mathrm{m}$ the displacement at the top of the column ($y = \ell$) are calculated and displayed in Figure 3 for different saturation degrees versus time. For the nearly saturated case $S_w = 0.9999$, the result coincides well with that of the saturated case [22]. For smaller water saturations, larger displacements and slower wave velocities are observed. It is also clear that no matter whether S_w is 0.5 or 0.9, the displacements and the wave velocities are nearly the same because the effective bulk modulus will not change too much for this range of the water saturation.

Similar results are found for the pore water pressure. In Figure 4, it is plotted versus time at the bottom of the column ($y = 0$) under the same stress boundary condition as above. The pore water pressure of the nearly saturated case ($S_w = 0.9999$) is very close to that of the saturated case, and the value is about 1.5 times larger than that created by the static Skempton effect.

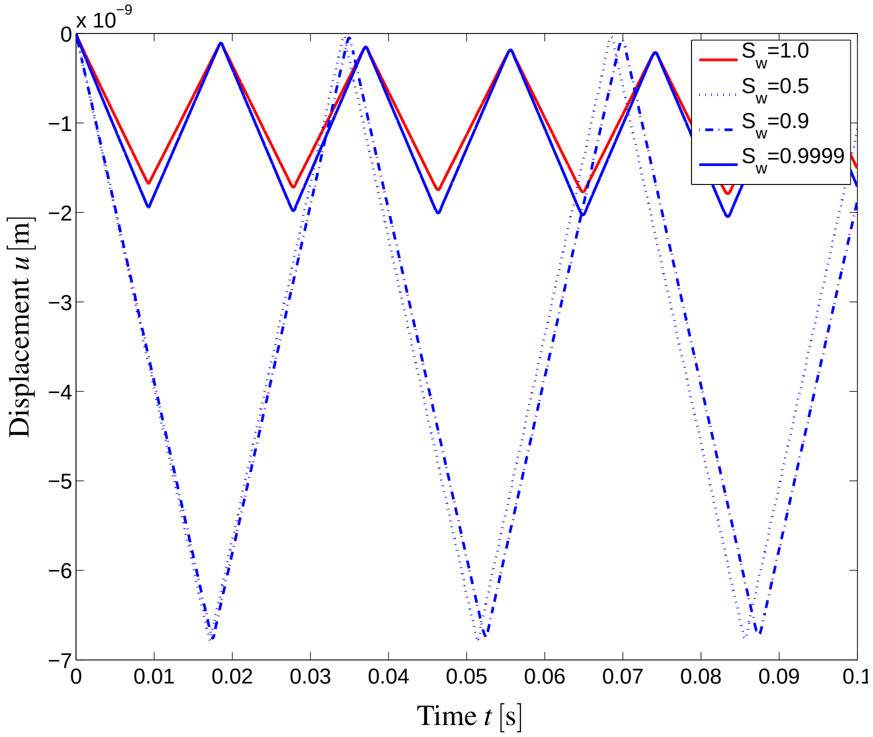

Figure 3: Displacement $u(t, y = \ell)$ versus time for different water saturation

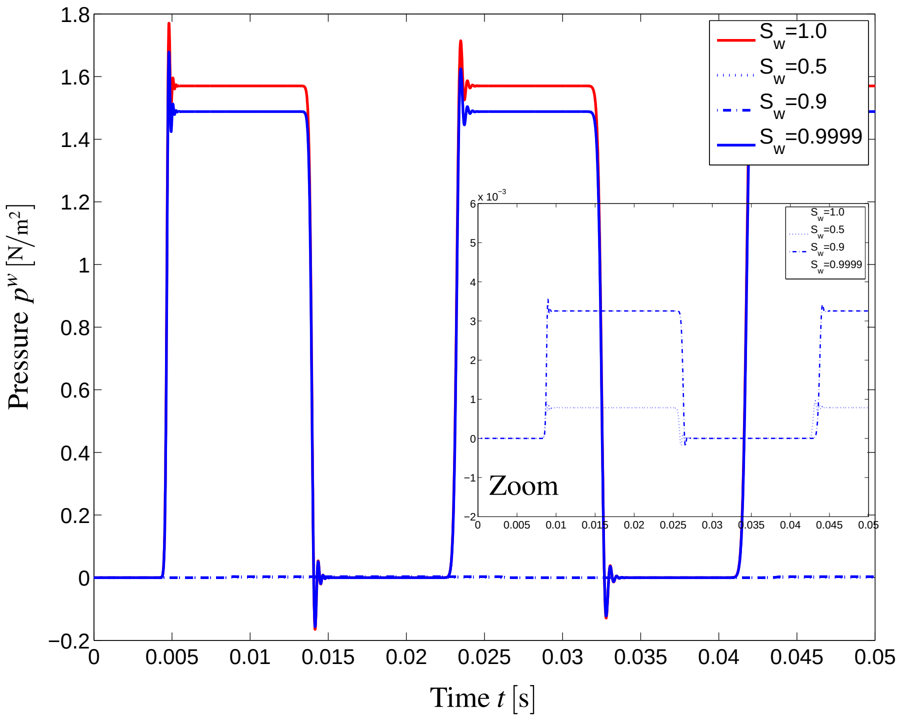

Figure 4: Pore water pressure $p^w(t, y = 0)$ versus time for different water saturation

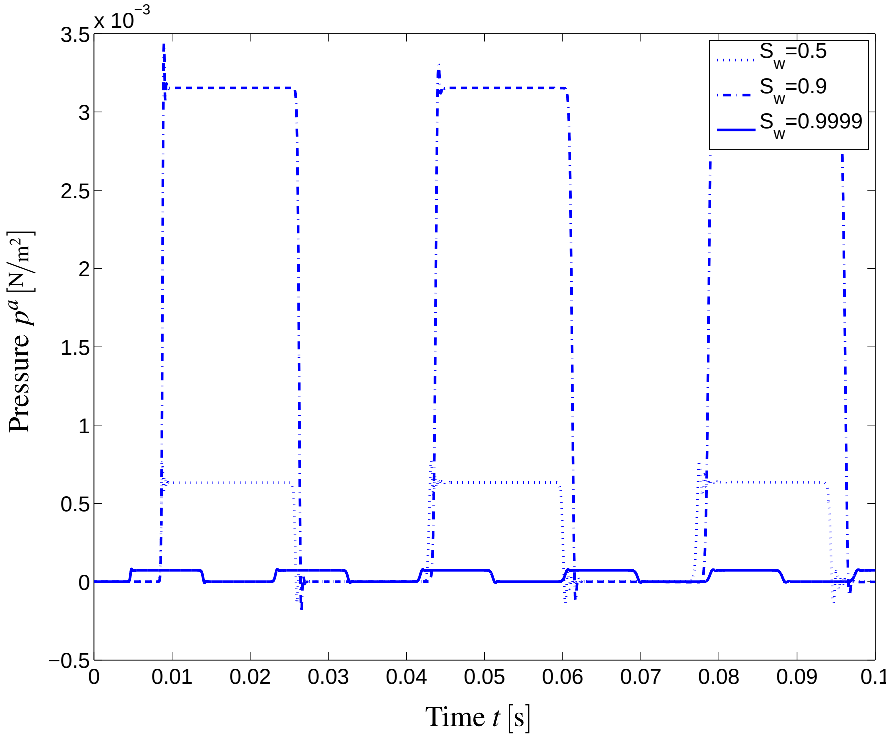

Figure 5: Pore air pressure $p^a(t, y=0)$ versus time for different water saturation

However, for smaller water saturations, the pore water pressure is very low (see the zoom in Figure 4).

The pore air pressure has much smaller values as displayed in Figure 5. Clearly, the smallest value of the pore air pressure is given for the nearly saturated case. By decreasing the saturation degree the pore air pressure is firstly increase and then decrease. It should be remarked that the oscillations at the jumps in the pressure solutions are numerical effects. They can not be avoided but changed by the time step size and the chosen multistep method.

In the figures shown above, it is impossible to detect the two slow waves due to the high attenuation. This can be overcome by reducing the viscosity artificially, i.e., two arbitrarily large permeabilities, $\kappa_w = 1.0 \times 10^3\,\mathrm{m^4/Ns}$ and $\kappa_a = 1.0 \times 10^3\,\mathrm{m^4/Ns}$ are chosen in the calculation. Further, because of the higher wave speed of the fast compressional wave several reflections would disturb the figure before the slow waves are visible. That is why an "infinite" column with a length $\ell = 1000\,\mathrm{m}$ is set and the pressures are observed thirty meters below the excitation point. The water saturation is set to $S_w = 0.99$ in the calculation.

As shown in Figure 6 and 7, the pore water pressure has two step jumps while the pore air pressure has three. This phenomenon can be rationalized as follows. For the pore water pressure, the first jump is the arrival of the fast wave. The second slow wave, arriving at a later time, is of negative amplitude and cancels the fast wave. However, the third slow wave can not be detected. For the pore air pressure, the fast wave and the second slow wave arrive at the same time as the waves for the pore water pressure. The difference is that the second slow wave is of positive

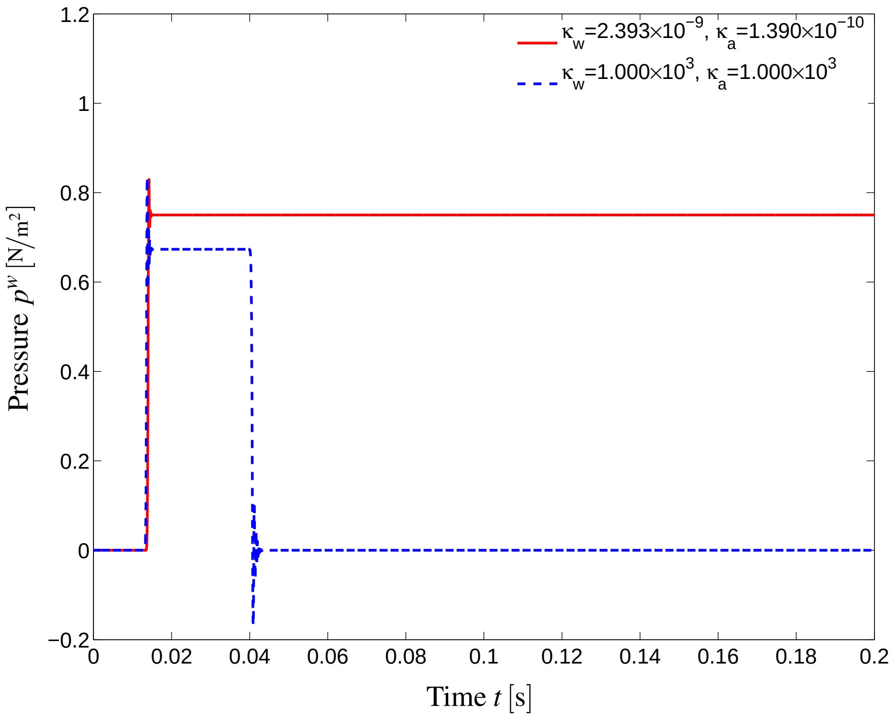

Figure 6: Pore water pressure p^w versus time for different κ_w and κ_a

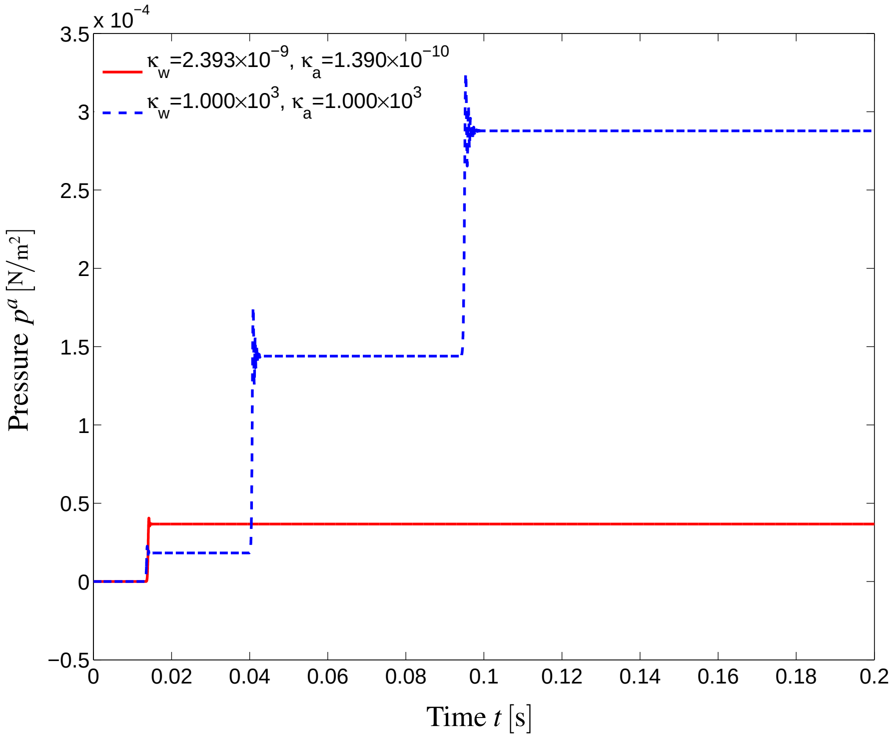

Figure 7: Pore air pressure $p^a(y = 970m)$ versus time for different κ_w and κ_a

amplitude and enlarges the fast wave. The third slow wave arriving at an even later time, is also of positive amplitude and keeps enlarging the overlapped waves.

As mentioned above, when calculating with the real permeabilities, for both the pore water and the pore air pressure, the slow waves are rapidly dissipated such that they have no effect when they arrive at the observation point. Therefore, only the arrival of the fast wave can be observed in experiments. Besides, the amplitude of the pore water pressure is slightly affected by changing the permeability. For the pore air pressure this is true only for the fast compressional wave whereas the amplitudes of the slow waves are strongly increasing with increasing the permeability.

Summarizing, there exist three compressional waves, however, for most natural materials the permeabilities may never become such large numbers that the slow compressional waves are visible.

5 Conclusions

Based on the theory of mixtures, an analytical solution in the Laplace domain for a partially saturated poroelastic one dimensional column has been deduced. The time domain solutions are obtained by with the convolution quadrature method. The solution of the fast wave velocity versus the water saturation coincides well with Biot-Gassmann's prediction and, hence, with Murphy's experiments (Massillon sandstone). The fast wave velocity will decrease with increasing the water saturation until the water saturation is very close to 1, then it will increase rapidly. Both of the two slow wave velocities have a turning point when the saturation degree is around 0.8 (0.85 for the second slow wave, 0.75 for the third slow wave), which reflect the different features for the fluid phase patterns. The attenuation of the fast wave is very small, while that of the two slow waves is very large, especially, that of the third slow wave. For the nearly saturated case, the partially saturated solution come close to the saturated solution. When decreasing the water saturation, the displacements become much larger, the pore water pressure decrease to very small values, and the pore air pressure first increase and then decrease. By assuming very large permeabilities of the fluids, the second and the third slow waves are observed with regard to the pore pressure. The third slow wave can only be observed in the pore air pressure result. For the realistic permeabilities of Massillion sandstone the two slow waves are highly damped and not visible in the results.

A Abreviations

In section 3, the following abbreviations are used:

$$B_1 = K + \frac{4}{3}G \quad B_2 = \rho - \beta S_w \rho_w - \gamma S_a \rho_a \quad B_3 = (\alpha - \beta) S_w \quad B_4 = (\alpha - \gamma) S_a$$

$$B_5 = \zeta S_{ww} S_w + \frac{n}{K_w} S_w - S_u \quad B_6 = \frac{\beta S_w}{\rho_w} \quad B_7 = \zeta S_{aa} S_w + S_u$$

$$B_8 = \zeta S_{ww} S_a + S_u \quad B_9 = \zeta S_{aa} S_a + \frac{n}{K_a} S_a - S_u \quad B_{10} = \frac{\gamma S_a}{\rho_a}$$

$$
\begin{aligned}
C_1 &= B_1 B_6 B_{10} \\
C_2 &= -(B_1 B_5 B_{10} + B_1 B_6 B_9 + B_2 B_6 B_{10} + B_3^2 B_{10} + B_4^2 B_6) \\
C_3 &= B_1(B_5 B_9 - B_7 B_8) + B_2(B_5 B_{10} + B_6 B_9) - B_3 B_4(B_7 + B_8) + B_3^2 B_9 + B_4^2 B_5 \\
C_4 &= B_2(B_7 B_8 - B_5 B_9)
\end{aligned}
$$

$$
N_1 = -\frac{C_2}{3C_1} \qquad N_2 = \frac{\sqrt[3]{2}}{N_3}
$$

$$
N_3 = \sqrt[3]{-2C_2^3 + 9C_1C_2C_3 - 27C_1^2C_4 + \sqrt{4(-C_2^2 + 3C_1C_3)^3 + (-2C_2^3 + 9C_1C_2C_3 - 27C_1^2C_4)^2}}
$$

B Analytical solutions for a 1d partially saturated poroelastic column

For the water pressure boundary condition ($\hat{u}(y=0)=0$, $\hat{\sigma}(y=\ell)=0$, $\hat{p}^w(y=\ell)=P^w$, $\hat{p}^a(y=\ell)=0$):

$$
\hat{u} = \frac{P^w}{Ms} \sum_{i=1}^{3} \left[\left(\frac{\alpha S_w}{K+4/3G} t_i + p_i \right) \frac{e^{\lambda_i s(y-\ell)} - e^{-\lambda_i s(y+\ell)}}{1+e^{-2\lambda_i s\ell}} \right] \tag{34a}
$$

$$
\hat{p}^w = \frac{P^w}{M} \sum_{i=1}^{3} \left[a_i \left(\frac{\alpha S_w}{K+4/3G} t_i + p_i \right) \frac{e^{\lambda_i s(y-\ell)} + e^{-\lambda_i s(y+\ell)}}{1+e^{-2\lambda_i s\ell}} \right] \tag{34b}
$$

$$
\hat{p}^a = \frac{P^w}{M} \sum_{i=1}^{3} \left[b_i \left(\frac{\alpha S_w}{K+4/3G} t_i + p_i \right) \frac{e^{\lambda_i s(y-\ell)} + e^{-\lambda_i s(y+\ell)}}{1+e^{-2\lambda_i s\ell}} \right] , \tag{34c}
$$

where $p_1 = b_2\lambda_3 - b_3\lambda_2$, $p_2 = b_1\lambda_3 - b_3\lambda_1$, $p_3 = b_2\lambda_1 - b_1\lambda_2$.
For the air pressure boundary condition ($\hat{u}(y=0)=0$, $\hat{\sigma}(y=\ell)=0$, $\hat{p}^w(y=\ell)=0$, $\hat{p}^a(y=\ell)=P^a$):

$$
\hat{u} = \frac{P_0^a}{Ms} \sum_{i=1}^{3} \left[\left(\frac{\alpha S_a}{K+4/3G} t_i + q_i \right) \frac{e^{\lambda_i s(y-\ell)} - e^{-\lambda_i s(y+\ell)}}{1+e^{-2\lambda_i s\ell}} \right] \tag{35a}
$$

$$
\hat{p}^w = \frac{P_0^a}{M} \sum_{i=1}^{3} \left[a_i \left(\frac{\alpha S_a}{K+4/3G} t_i + q_i \right) \frac{e^{\lambda_i s(y-\ell)} + e^{-\lambda_i s(y+\ell)}}{1+e^{-2\lambda_i s\ell}} \right] \tag{35b}
$$

$$
\hat{p}^a = \frac{P_0^a}{M} \sum_{i=1}^{3} \left[b_i \left(\frac{\alpha S_a}{K+4/3G} t_i + q_i \right) \frac{e^{\lambda_i s(y-\ell)} + e^{-\lambda_i s(y+\ell)}}{1+e^{-2\lambda_i s\ell}} \right] , \tag{35c}
$$

where $q_1 = a_3\lambda_2 - a_2\lambda_3$, $q_2 = a_3\lambda_1 - a_1\lambda_3$, $q_3 = a_1\lambda_2 - a_2\lambda_1$.
For the displacement boundary condition ($\hat{u}(y=0)=U_0$, $\hat{\sigma}(y=\ell)=0$, $\hat{p}^w(y=\ell)=0$, $\hat{p}^a(y=$

$\ell) = 0$):

$$\hat{u} = \frac{U_0}{N}\sum_{i=1}^{3}\left[(e_i\rho_w + f_i\rho_a + g_it_i)\frac{e^{\lambda_i s(y-2\ell)} + e^{-\lambda_i sy}}{1+e^{-2\lambda_i s\ell}}\right] \tag{36a}$$

$$\hat{p}^w = \frac{U_0}{N}\sum_{i=1}^{3}\left[(e_i\rho_w + f_i\rho_a + g_it_i)a_is\frac{e^{\lambda_i s(y-2\ell)} - e^{-\lambda_i sy}}{1+e^{-2\lambda_i s\ell}}\right] \tag{36b}$$

$$\hat{p}^a = \frac{U_0}{N}\sum_{i=1}^{3}\left[(e_i\rho_w + f_i\rho_a + g_it_i)b_is\frac{e^{\lambda_i s(y-2\ell)} - e^{-\lambda_i sy}}{1+e^{-2\lambda_i s\ell}}\right], \tag{36c}$$

where $e_1 = b_3\lambda_3 - b_2\lambda_2$, $e_2 = b_1\lambda_1 - b_3\lambda_3$, $e_3 = b_2\lambda_2 - b_1\lambda_1$, $f_1 = a_2\lambda_2 - a_3\lambda_3$, $f_2 = a_3\lambda_3 - a_a\lambda_1$, $f_3 = a_1\lambda_1 - a_2\lambda_2$, $g_1 = \lambda_2\lambda_3$, $g_2 = \lambda_1\lambda_3$, $g_3 = \lambda_1\lambda_2$, $N = \lambda_2\lambda_3t_1 + \lambda_1\lambda_3t_2 + \lambda_1\lambda_2t_3$.

References

[1] B. Albers. Analysis of the propagation of sound waves in partially saturated soils by means of a macroscopic linear poroelastic model. *Transp. Porous Media*, 80(1), 2009.

[2] B. Albers. *Modeling and Numerical Analysis of Wave Propagation in Saturated and Partially Saturated Porous Media*. Shaker Verlag, Berlin, 2010.

[3] C.G. Bao, B.W. Gong, and L.T. Zhan. Properties of unsaturated soils and slope stability of expansive soils. In *Second International Conference on Unsaturated Soils*. International Academic Publishers, 1998.

[4] J. G. Berryman. Waves in partially saturated porous media. In W. E. Fitzgibbon and M. F. Wheeler, editors, *Wave Propagation and Inversion*, pages 1–25. SIAM, Philadelphia, 1992.

[5] M. A. Biot. Theory of propagation of elastic waves in a fluid-saturated porous solid.I. Low-frequency range. *J. Acoust. Soc. Am.*, 28(2):168–178, 1956.

[6] M. A. Biot. Theory of propagation of elastic waves in a fluid-saturated porous solid.II. Higher frequency range. *J. Acoust. Soc. Am.*, 28(2):179–191, 1956.

[7] R. H. Brooks and A. T. Corey. Hydraulic properties of porous media. In *Hydraulic Papers*. Colorado State Univ., 1964.

[8] R. de Boer. *Theory of Porous Media*. Springer-Verlag, Berlin, 2000.

[9] S. K. Garg, A. H. Nafeh, and A. J. Good. Compressional waves in fluid-saturated elastic porous media. *J. Appl. Phys.*, 45(5):1968–1974, 1974.

[10] F. Gassmann. Über die Elastizität poröser Medien. *Viertel. Naturforsch. Ges. Zürich*, 96 (1):1–23, 1951.

[11] B. Gatmiri and E. Jabbari. Time-domain Green's functions for unsaturated soils. Part I: Two-dimensional solution. *Internat. J. Solids Structures*, 42:5971–5990, 2005.

[12] B. Gatmiri and E. Jabbari. Time-domain Green's functions for unsaturated soils. Part II: Three-dimensional solution. *Internat. J. Solids Structures*, 42:5991–6002, 2005.

[13] R. W. Lewis and B. A. Schrefler. *The Finite Element Method in the Static and Dynamic Deformation and Consolidation of Porous Media*. John Wiley and Sons, Chichester, 1998.

[14] K. K. Muraleetharan and C. Wei. Dynamic behaviour of unsaturated porous media: Governing equations using the theory of mixtures with interfaces (TMI). *Int. J. Numer. Anal. Methods Geomech.*, 23(13):1579–1608, 1999.

[15] W.F. Murphy. Effects of partial water saturation on attenuation in Massilon sandstone and Vycor porous glass. *J. Acoust. Soc. Am.*, 71, 1982.

[16] W.F. Murphy. Acoustic measures of partial gas saturation in tight sandstones. *J. Geophys. Res.*, 89(B13), 1984.

[17] A. J. Philippacopoulos. Waves in partially saturated medium due to surface loads. *J. Engrg. Mech., ASCE*, 114(10):1740–1759, 1988.

[18] T.J. Plona. Observation of a second bulk compressional wave in porous medium at ultrasonic frequencies. *Appl. Phys. Lett.*, 36(4), 1980.

[19] N. Ravichandran and K. K. Muraleetharan. Dynamics of unsaturated soils using various finite element formulations. *Int. J. Numer. Anal. Methods Geomech.*, 33(5):611–631, 2009.

[20] M. Schanz. *Wave Propagation in Viscoelastic and Poroelastic Continua: A Boundary Element Approach*, volume 2 of *Lecture Notes in Applied Mechanics*. Springer-Verlag, Berlin, Heidelberg, New York, 2001.

[21] M. Schanz. Poroelastodynamics: Linear models, analytical solutions, and numerical methods. *AMR*, 62(3):030803–1–030803–15, 2009.

[22] M. Schanz and A. H.-D. Cheng. Transient wave propagation in a one-dimensional poroelastic column. *Acta Mech.*, 145(1-4):1–18, 2000.

[23] B. A. Schrefler and R. Scotta. A fully coupled dynamic model for two-phase fluid flow in deformable porous media. *Comput. Methods Appl. Mech. Engrg.*, 190(24–25), 2001.

[24] D. Smeulders, J. De La Rosette, and M. Van Dongen. Waves in partially saturated porous media. *Transp. Porous Media*, 9(1–2), 1992.

[25] M. Th. van Genuchten. A closed-form equation for predicting the hydraulic conductivity of unsaturated soils. *Soil Sci. Soc. Am. J*, 44, 1980.

[26] I. Vgenopoulou and D. E. Beskos. Dynamics of saturated rocks. IV: Column and borehole problems. *J. Engrg. Mech., ASCE*, 118(9):1795–1813, 1992.

[27] C. Wei and K. K. Muraleetharan. A continuum theory of porous media saturated by multiple immiscible fluids: I. Linear poroelasticity. *Int. J. Engng. Sci.*, 40(16):1807–1833, 2002.

[28] C. Wei and K. K. Muraleetharan. A continuum theory of porous media saturated by multiple immiscible fluids: II. Lagrangian description and variational structure. *Int. J. Engng. Sci.*, 40(16):1835–1854, 2002.

[29] K. Wilmanski. Elastic modelling of surface waves in single and multicomponent systems. In C. G. Lai and K. Wilmanski, editors, *Surface Waves in Geomechanics: Direct and Inverse Modelling for Soils and Rocks*, volume 481 of *CISM*, chapter 5, pages 203–276. Springer-Verlag, Wien, 2005.

[30] R. K. Wilson and E. C. Aifantis. On the theory of consolidation with double porosity. *Int. J. Engng. Sci.*, 20:1009–1035, 1982.

[31] O. C. Zienkiewicz, A. H. C. Chan, M. Pastor, D. K. Paul, and T. Shiomi. Static and dynamic behaviour of soils: A rational approach to quantitative solutions. I. fully saturated problems. *Proc. R. Soc. Lond. A*, 429(1877):285–309, 1990.